Electronic Supplementary Material (ESI) for Journal of Materials Chemistry B.
This journal is © The Royal Society of Chemistry 2023

Electronic Supplementary Material

Supramolecular Detoxification of Nitrogen Mustard via Host-guest Encapsulation by Carboxylatopillar[5]arene

Siyuan Zhou, [a,#] Yi Chen, [a,#] Jie Xu,[c] Yongfei Yin, [a] Jianqing Yu, [c] Wei Liu, *[b] Shigui Chen*[a] and Lu Wang,* [a]

[a]The Institute for Advanced Studies, and Department of Gastroenterology, Hubei Clinical Center & Key Lab of Intestinal & Colorectal Diseases, Zhongnan Hospital, Wuhan University, Wuhan, Hubei 430072, P. R. China
[b]Department of Ophthalmology, Union Hospital, Tongji Medical College, Huazhong University of Science and Technology, Wuhan 430022, P. R. China
[c] School of Pharmaceutical Sciences, Wuhan University, 185 Donghu Road, Wuhan, Hubei 430072, P. R. China

Email: weiliu0113@hust.edu.cn (Wei Liu), sgchen@whu.edu.cn (Shigui Chen), wanglu-027@whu.edu.cn (Lu Wang).

Table of Contents

General methods and materials.....S3-S4
Synthetic Procedures S4-S6
Supporting results and experimental raw data.....S6
Figure S1. The section of the ^{1}H NMR spectra of **NM·HCl** with **P5A** at an initial concentration of 5.0 mM in D_2O. S6
Figure S2. Sections of ^{1}H NMR titration spectra of **P5A** with **NM·HCl**.....S6
Figure S3. The observed ^{1}H NMR chemical shifts of protons in **P5A**.....S7
Figure S4. Nonlinear least-squares analysis of **NM·HCl ⊂ P5A** complex.....S8
Figure S5. The optimal structure of **P5A**, **NM** and the complex **NM ⊂ P5A** S8
Figure S6. ESP surfaces of **P5A**, **NM** and the complex **NM ⊂ P5A** S8
Figure S7. The Noncovalent interaction graphs of the complex **NM ⊂ P5A**. S9
Figure S8. ^{1}H NMR spectrum of **NM** in D_2O (600 MHz, 298.0 K). S9
Figure S9. The degradation of **NM** and **2** in H_2O. S10
Figure S10. The section of the ^{1}H NMR spectra of **2** at an initial concentration of 5.0 mM in D_2O.....S10
Figure S11. The section of the ^{1}H NMR spectra of **2** at an initial concentration of 10.0 mM in D_2O.....S10
Figure S12. The section of the ^{1}H NMR spectra of **2** with **CP[5]AK** at an initial concentration of 5.0 mM in D_2O.. .....S11
Figure S13. Sections of ^{1}H NMR titration spectra of **2** with **CP[5]AK** (0.10-8.10 equiv.) in D_2O S11
Figure S14. Sections of ^{1}H NMR titration spectra of **CP[5]AK** with **2** (0.20-5.70 equiv.) in D_2O S12
Figure S15. The observed ^{1}H NMR chemical shifts of protons in **CP[5]AK**. S12
Figure S16. Nonlinear least-squares analysis of **2⊂ CP[5]AK** complex.....S13
Table S1. Thermodynamic parameters of the binding of **CP[5]AK** with **2**. S13
Figure S17. ITC of **CP[5]AK** with **2**(in H_2O, pH=8.8, 10 °C). S13
Figure S18. ITC of **CP[5]AK** with **2**(in H_2O, pH=8.8, 37 °C). S14
Figure S19. ITC of **CP[5]AK** with **2**(in PBS, pH=7.4, 25 °C). S14
Figure S20. Monoalkylation of guanine disodium nucleotide by **2**. S14
Figure S21. The section of the ^{1}H NMR spectra of **GMP** disodium salt in the presence of **NM** (1.0 equiv.) ..S15
Figure S22. The section of the ^{1}H NMR spectra of **GMP** disodium salt and **NM** in the presence of **CP[5]AK** (1.0 equiv.). S15
Figure S23. The section of the ^{1}H NMR spectra of **GMP** disodium salt and **NM** in the presence of **CP[5]AK** monomer (5.0 equiv.).....S16
Figure S24. The section of the ^{1}H NMR spectra of **GMP** disodium salt and **NM** in the presence of **CP[5]AK** (0.5 equiv.). S16
Figure S25. The content of **GMP** disodium salt with time in different experimental groups.. .....S17
Figure S26. vitro cytotoxicity studies (CHO cells).....S17
Figure S27. vitro cytotoxicity studies (HSC-T6 cells).....S18
Figure S28. ^{1}H NMR spectrum (D_2O, 298 K, 600 MHz) of **CP[5]AK**. S18
Figure S29. ^{13}C NMR spectrum (D_2O, 298 K, 600 MHz) of **CP[5]AK**.....S19
Figure S30. MALDI-TOF mass spectrum of **CP[5]AK** [M-10K^++9H^+]$^-$**.** S19
References S20

General methods and materials

All solvents were dried before use following the standard procedures. Unless indicated otherwise, all starting materials were obtained from commercial suppliers and used without additional purification. Analytical thin-layer chromatography (TLC) was performed on silica-gel plates w/UV254. ^{1}H NMR and ^{13}C NMR spectra were recorded with a Bruker BIOSPIN AV 600 NMR instrument at 600 MHz (^{1}H) and 125 MHz (^{13}C) and JEOL JNM-ECZ400 spectrometer at 400 MHz (^{1}H) and 100 MHz (^{13}C) in the indicated solvents at 25 °C. Chemical shifts are expressed in parts per million (δ, ppm) using residual solvent protons as internal standard (^{1}H NMR δ (ppm) for $CDCl_3$ = 7.26, DMSO-d_6 = 2.50 and D_2O = 4.79; ^{13}C NMR δ (ppm) for $CDCl_3$ = 77.16 and DMSO-d_6 = 39.52). ITC data was collected on a Malvern Microcal PEAQ-ITC instrument.

Computational details

The ground state geometries were derived by density functional theory (DFT). All the computations were performed using the Gaussian 09 program on a personal computer using B3LYP in conjunction with 6-31G (d, p). All analyses as well as drawing of various kinds of maps were finished using the Multiwfn 3.7 code.[1-2] In addition to an energy optimized structure, the electron densities of the targeted compounds were investigated using electrostatic potential (ESP) and noncovalent interactions (NCIs).

Internal Standard Method

In the monitoring process, the solution of 4-aminopyridine (in D_2O, 100 mM) was sealed in the capillary as internal standard. Since the 4-aminopyridine sealed in the capillary does not affect the hydrolysis process of **NM**, and the integral area remains unchanged during the whole monitoring process. The NMR integral was converted to the concentration and a curve of the concentration of compound **2** was obtained as a function of time.

Cell culture

CHO cells and HSC-T6 cells were incubated in complete culture medium comprising DMEM supplemented with 10% FBS, 100 IU/mL penicillin and 100 mg/mL streptomycin, and then cultured at 37 °C in a humidified atmosphere with 5% CO_2. The attached cells were routinely passaged treatment with a 0.25% trypsin-EDTA solution after reaching 80% confluency. The medium was refreshed every 3 days.

***In vitro* cytotoxicity assay of NM and CP[5]AK**

The cytotoxicity of NM and **CP[5]AK** against chinese hamster ovary (CHO) cells and hepatic stellate (HSC-T6) cells was then evaluated using MTT assay based on the manufacturer's instructions. In brief, CHO cells and HSC-T6 cells were seeded in 96-well plates at an appropriate density of 3 × 10^3 cells per well and then cultured with **NM** and **CP[5]AK** of different concentrations for 48 h. Then MTT solution (20 μL, 5 mg/mL) was added into complete culture medium for 4 h, and then poured out the medium in the 96-well plate. the medium was added with DMSO solution (100 μL). When completely dissolved, the absorbance was measured at a wavelength of 570 nm with a microplate reader (Bio-Tek, Synergy H1, USA).

Animal experiment

Kunming mice (6–8 weeks) were obtained from Laboratory Animal Centre of Hubei, China. The animal protocols were approved by the Institutional Animal Care and Use Committee, Tongji Medical College, Huazhong University of Science and Technology, and in line with

the protection guidelines of animal subjects. Animal ethics have been permitted by the regulations of the Institutional Animal Care and Use Committee, Tongji Medical College, Huazhong University of Science and Technology.

Exposure to NM and Administration of CP[5]AK

Mice were randomly divided into 4 groups:

Nitrogen mustard group

The depilated skin of the mice was dripped with **NM** in acetone (100 μL, 20 mg/mL). The skin changes of the infected mice were recorded after 1 h, 8 h, 12 h, 24 h, 32 h, 48 h, 56 h, 60 h, 72 h, 80 h, 96 h, 104 h and 108 h by pictures.

Control group

The depilated skin of the mice was dripped with acetone (100 μL).

CP[5]AK treatment group

The depilated skin of the mice was dripped with **NM** in acetone (100 μL, 20 mg/mL). Then **CP[5]AK** (20 μL, 0.3 M) in aqueous solution was added to the affected area at 1 h, 8 h, 12 h, 24 h, 32 h, 48 h, 56 h, 60 h, 72 h, 80 h, 96 h, 104 h, 108 h, respectively. The skin changes of mice exposed to **NM** were recorded by pictures.

CP[5]AK monomer treatment group

The depilated skin of the mice was dripped with **NM** in acetone (100 μL, 20 mg/mL). Then **CP[5]AK** monomer (20 μL, 0.3 M) in aqueous solution was added to the affected area at 1 h, 8 h, 12 h, 24 h, 32 h, 48 h, 56 h, 60 h, 72 h, 80 h, 96 h, 104 h, 108 h, respectively. The skin changes of mice exposed to **NM** were recorded by pictures.

Synthetic Procedures:

Compound **3**[3], **5**[4] were synthesized following already reported protocol (Scheme S1-2).

Scheme S1. Synthesis of **CP[5]AK 3**.

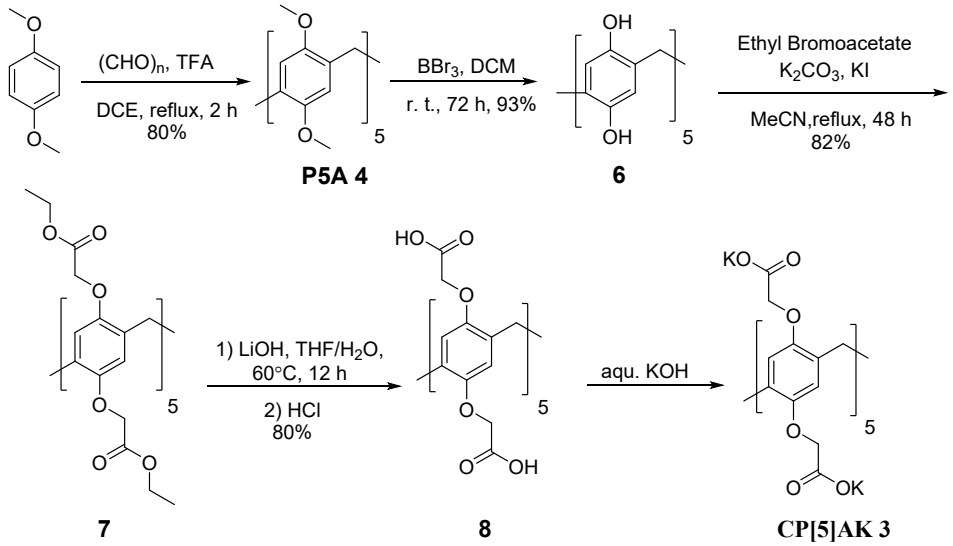

P5A 4: 1,4-Dimethoxybenzene (13.8 g, 100.0 mmol) was suspended in dichloroethane (950 mL). Paraformaldehyde (3.0 g, 100.0 mmol) was added to the suspension, which was then stirred for 10 min. Upon the addition of trifluoroacetic acid (50 mL), the reaction mixture was refluxed for 2 h and then quenched by the addition of ethanol (1000 mL). The resulting yellow-green precipitate was collected by filtration. The crude product was

recrystallized from $CHCl_3$ to yield 12.0 g (80 %) of **P5A 4** as a white powder. ^{1}H NMR (400 MHz, $CDCl_3$): δ 6.76 (s, 10H), 3.78 (s, 10H), 3.65 (s, 30H).

Compound **6: 4** (1.5 g, 2.0 mmol) was dissolved in anhydrous CH_2Cl_2 (50 mL). BBr_3 (25.0 g, 100.0 mmol) was then added slowly under ice bath, and the resulting mixture was stirred at room temperature for further 72 h. Water (100 mL) was then added and the reaction mixture was stirred for 24 h at room temperature. The resulting precipitate was filtered and washed with water which gave 1.1 g (93 %) of compound **6** as a white solid. ^{1}H NMR (400 MHz, $(CD_3)_2CO$): δ 8.08 (s, 10H), 6.67 (s, 10H), 3.59 (s, 10H). ^{13}C NMR (100 MHz, $(CD_3)_2CO$): δ 143.80, 128.02 118.28, 30.65.

Compound **7:** Compound **6** (0.61 g, 1.0 mmol) was suspended in MeCN (50 mL) and K_2CO_3 (6.9 g, 50.0 mmol) was added. The suspension was stirred for 30 min at room temperature, then KI (0.1 g) and ethyl bromoacetate (8.4 g, 50.0 mmol) were added. The mixture was refluxed for 48 h, and then the filtrate was collected and followed by the removal of organic solvent in vacuum. The crude product was purified by silica chromatography (CH_2Cl_2/Me_2CO, 100:0 to 10:1) to yield 1.2 g (82 %) of compound **7** as a white solid. ^{1}H NMR (400 MHz, $CDCl_3$): δ 7.04 (s, 10H), 4.53 (q, *J* = 15.7 Hz, 20H), 4.07 (m, 20H), 3.85 (s, 10H), 0.97 (t, *J* = 7.1 Hz, 30H).

Compound **8:** Compound **7** (0.74 g, 0.5 mmol) was dissolved in THF (10 mL), followed by the addition of aqueous LiOH solution (5 mL, 20%). The mixture was heated to 60 °C for 12 h. After cooling to room temperature, the mixture was acidified with HCl. The resulting precipitate was collected by filtration, washed with water, and dried under vacuum to yield 0.48 g (80%) of Compound **8** as a white solid. ^{1}H NMR (400 MHz, DMSO-d_6): δ 12.97 (s, 10H), 7.10 (s, 10H), 4.67 (d, *J* = 15.8, 10H), 4.41 (d, *J* = 15.8, 10H), 3.73 (s, 10H).

CP[5]AK 3: To prepare a standard D_2O solution of **CP[5]AK** (20.0 mM), compound **8** (10.0 mg, 0.0084 mmol) was suspended in D_2O (0.34 mL) followed by the addition of 1.0 M solution of KOH (0.084 mL, 0.084 mmol). ^{1}H NMR (600 MHz, DMSO-d_6) δ 6.73 (s, 10H), 4.31 (s, 20H), 3.83 (s, 10H). ^{13}C NMR (125 MHz, DMSO-d_6) δ 177.5, 149.2, 128.5, 114.4, 67.6, 29.0. MALDI-TOF-MS: calcd for $C_{55}H_{40}O_{30}9H^-$ $[M-10K^+ +9H^+]^-$ 1189.2314; found 1189.23174.

Scheme S2. Synthesis of **8**.

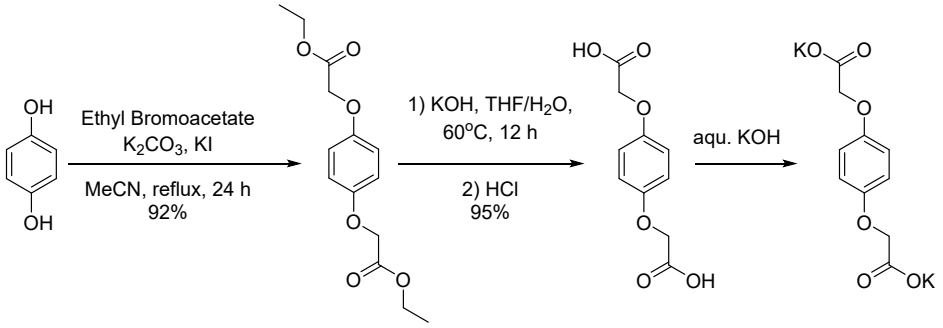

Compound 9: Hydroquinone (1.1 g, 10 mmol) was dissolved in MeCN (50 mL) and K_2CO_3 (6.9 g, 50 mmol) was added. The resulting mixture was stirred for 30 min at room temperature, then KI (0.1 g) and ethyl bromoacetate (2.5 g, 15 mmol) was added. The mixture was refluxed for 24 h, and then the filtrate was collected and followed by the

removal of organic solvent in vacuum. The crude product was purified by silica chromatography (PE/EA, 10:1 to 1:1) to obtain 2.6 g (92 %) of compound **9** as a white solid. ^{1}H NMR (400 MHz, $CDCl_3$): δ 6.85 (s, 4H), 4.56 (s, 4H), 4.26 (q, *J* = 7.1 Hz, 4H), 1.29 (t, *J* = 7.1 Hz, 4H).

Compound 10: Aqueous KOH solution (10 mL, 20%) was added into a solution of compound **9** (1.4 g, 5 mmol) in THF (10 mL). The mixture was heated to 60 °C for 12 h. After cooling to room temperature, the mixture was acidified with HCl. The resulting precipitate was collected by filtration, washed with water, and dried under vacuum to yield 1.1 g (95 %) of compound **10** as a white solid. ^{1}H NMR (400 MHz, DMSO-d_6): δ 6.83 (s, 4H), 4.59 (s, 4H).

Compound 8: To prepare a standard D_2O solution of **5** (100.0 mM), compound **10** (100.0 mg, 0.442 mmol) was suspended in D_2O (3.541 mL) followed by the addition of 1.0 M solution of KOH (0.884 mL, 0.884 mmol). ^{1}H NMR (400 MHz, D_2O): δ 6.86 (s, 4H), 4.40 (s, 4H).

Supporting results and experimental raw data

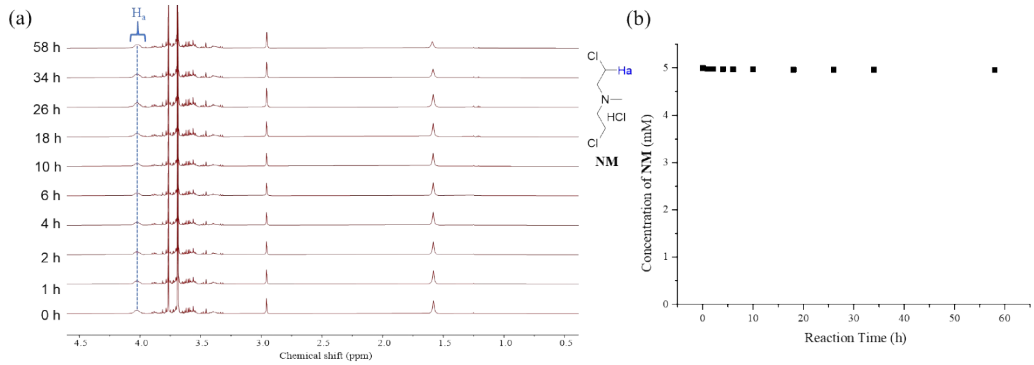

Figure S1. (a) The section of the ^{1}H NMR spectra (600 MHz, 298 K) of **NM·HCl** and **P5A** at an initial concentration of 5.0 mM in $CDCl_3$ at different time and (b) the plot of the concentration of **NM·HCl** as a function of time.

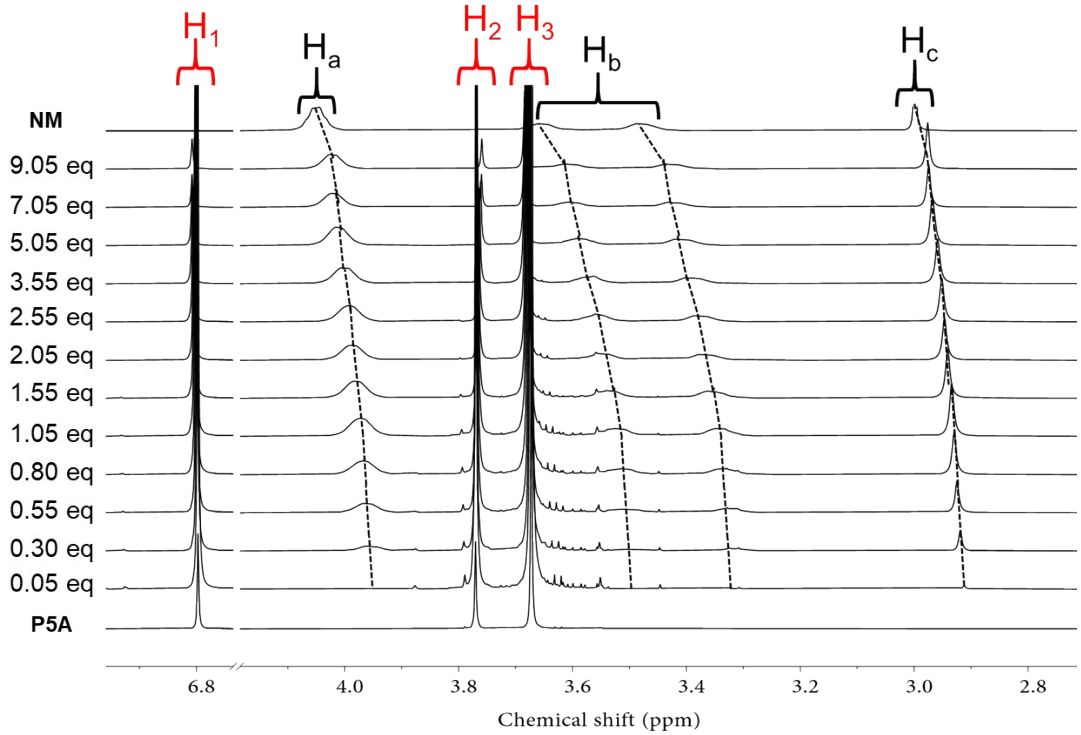

Figure S2. Sections of ^{1}H NMR spectra (600 MHz, 298 K) of a solution of **P5A** (10.0 mM in $CDCl_3$) obtained upon an incremental addition of **NM·HCl** (0.05-9.05 equiv.) in $CDCl_3$.

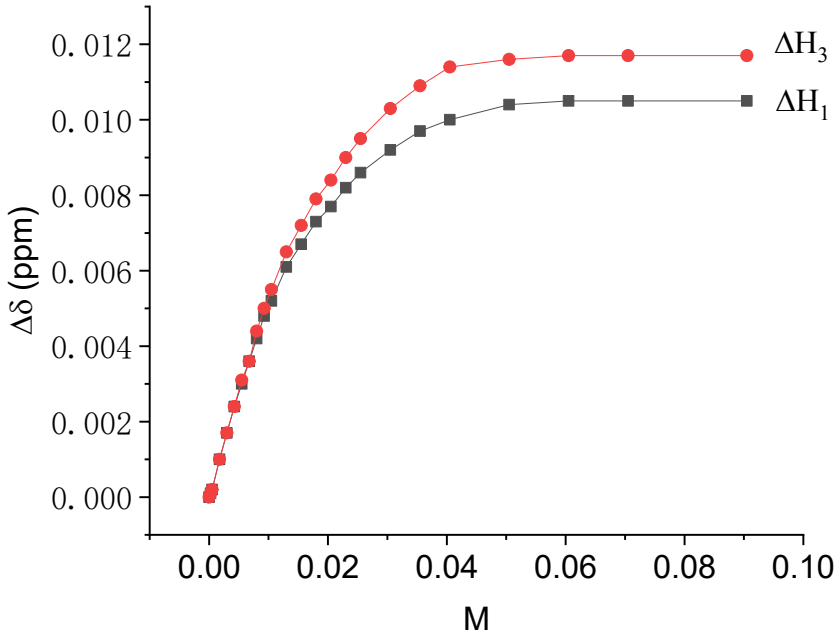

Figure S3. The observed ^{1}H NMR chemical shifts ($\Delta\delta = \delta_{observed} - \delta_{free}$ ppm) of protons in **P5A**.

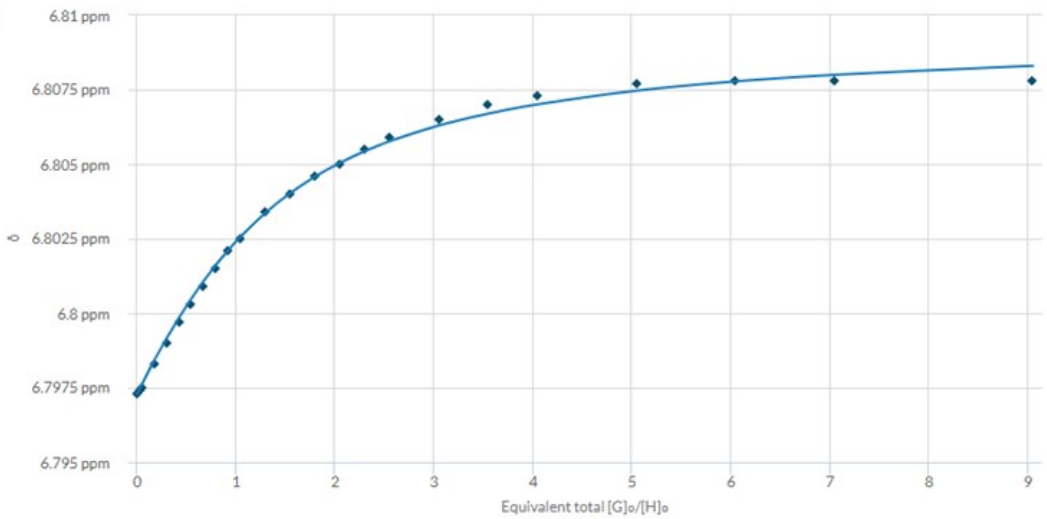

Figure S4. Non-linear least-squares fitting of the chemical shift changes of H during titration experiments of **P5A** with **NM·HCl**. The chemical shift of $\mathbf{H_1}$ was fitted to a 1:1 (host : guest) binding model to give K_a = 1.27 × 10^2 M^{-1}. All solid lines were obtained from non-linear curve-fitting with the Nelder-Mead method to a 1:1 binding model using the http://supramolecular.org/ web applet.

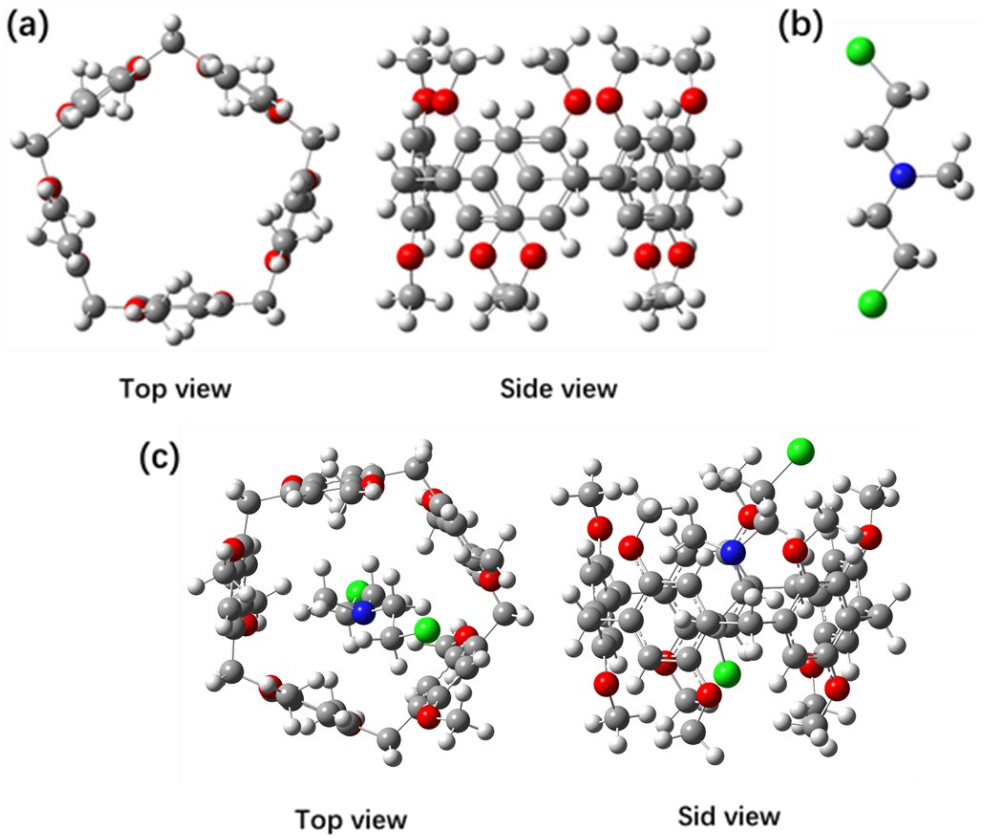

Figure S5. The optimal structure of (a) **P5A**, (b) **NM** and (c) the complex **NM** ⊂ **P5A**.

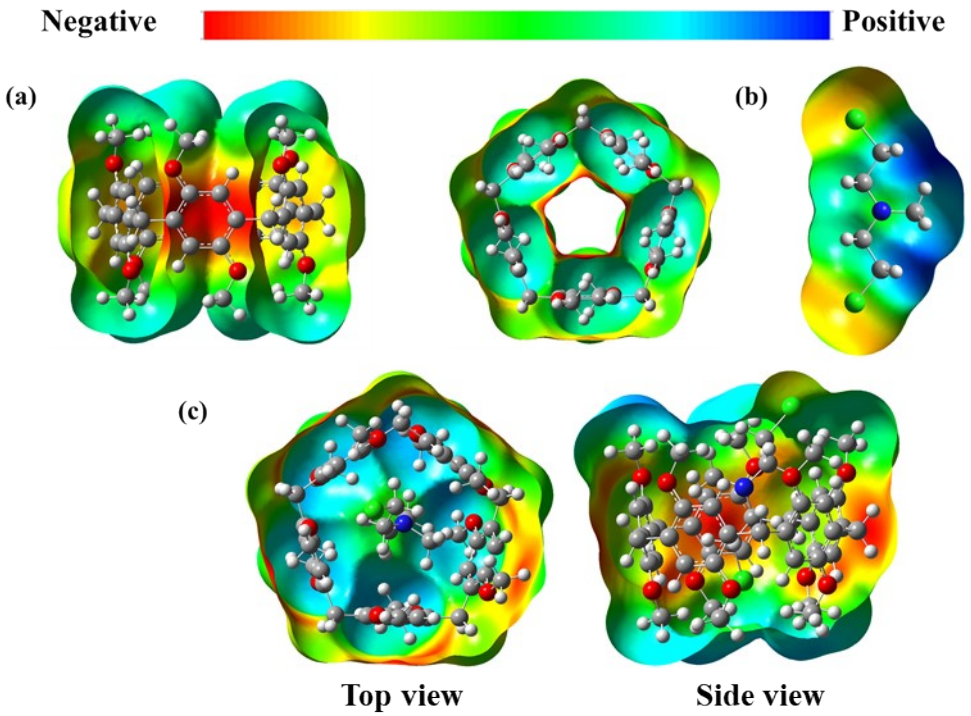

Figure S6. Molecular electrostatic potential (ESP) surfaces of (a) **P5A**, (b) **NM** and (c) the complex **NM** ⊂ **P5A**.

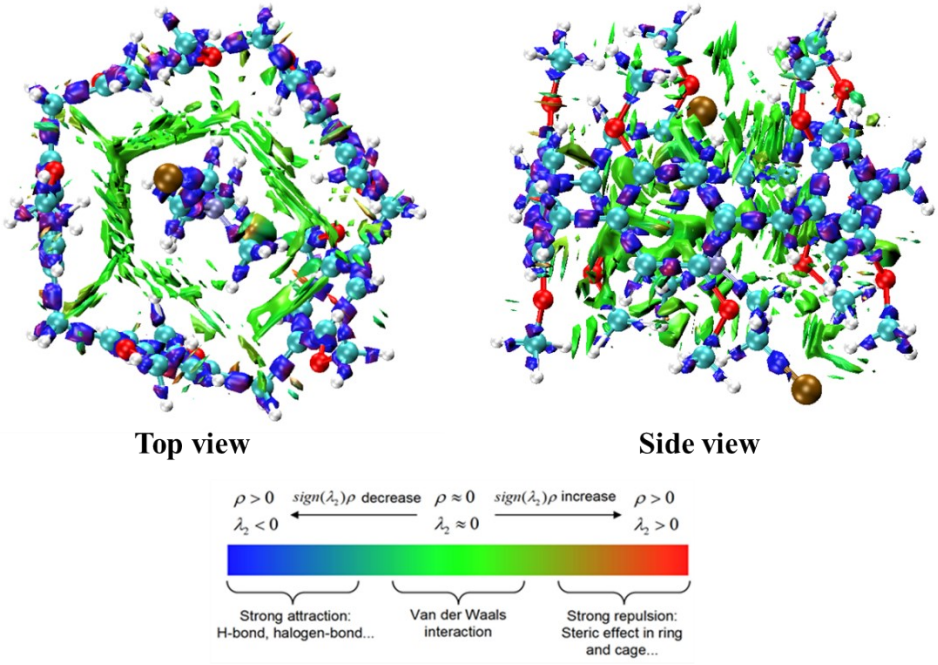

Figure S7. The Noncovalent interaction graphs of the complex **NM**⊂**P5A**.

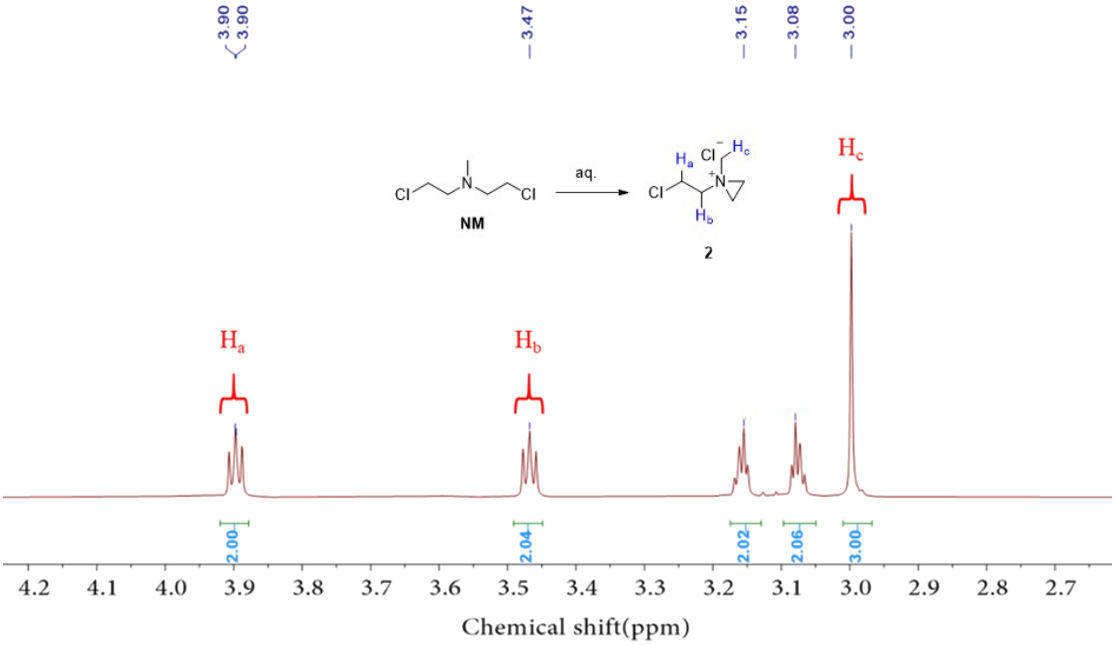

Figure S8. ^{1}H NMR spectrum of **NM** in D_2O (600 MHz, 298 K).

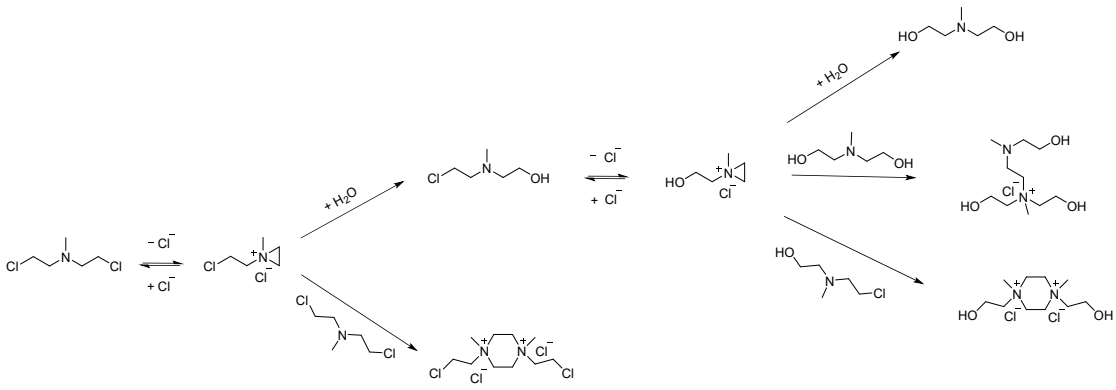

Figure S9. The degradation of **NM** and **2** in H_2O.

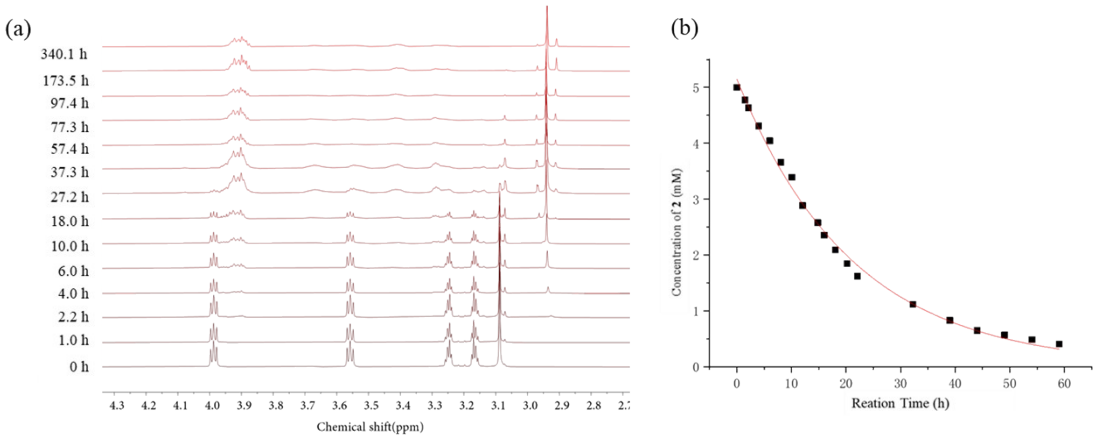

Figure S10. (a) The section of the ^{1}H NMR spectra (600 MHz, 298 K) of **2** at an initial

concentration of 5.00 mM in D_2O at different time and (b) the plot of the concentration of **2** as a function of time.

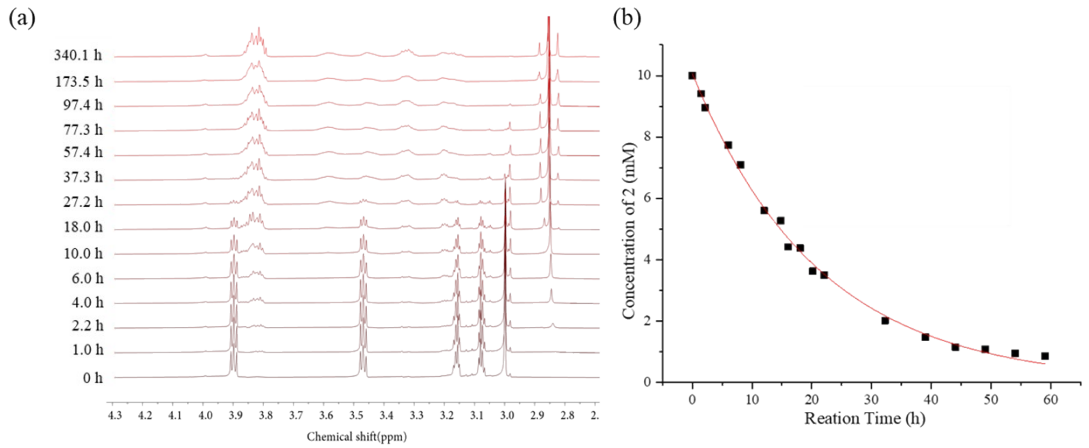

Figure S11. (a) The section of the ^{1}H NMR spectra (600 MHz, 298 K) of **2** at an initial concentration of 10.0 mM in D_2O at different time and (b)the plot of the concentration of **2** as a function of time.

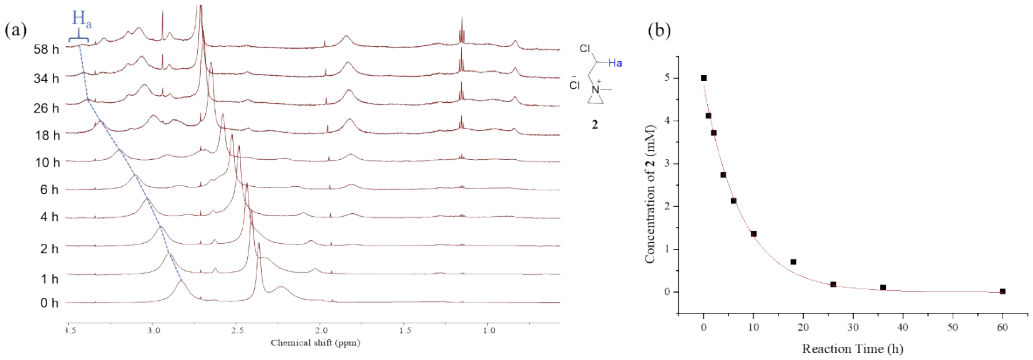

Figure S12. (a) The section of the ^{1}H NMR spectra (600 MHz, 298 K) of **2** and **CP[5]AK** at an initial concentration of 5.0 mM in D_2O at different time and (b) the plot of the concentration of **2** as a function of time.

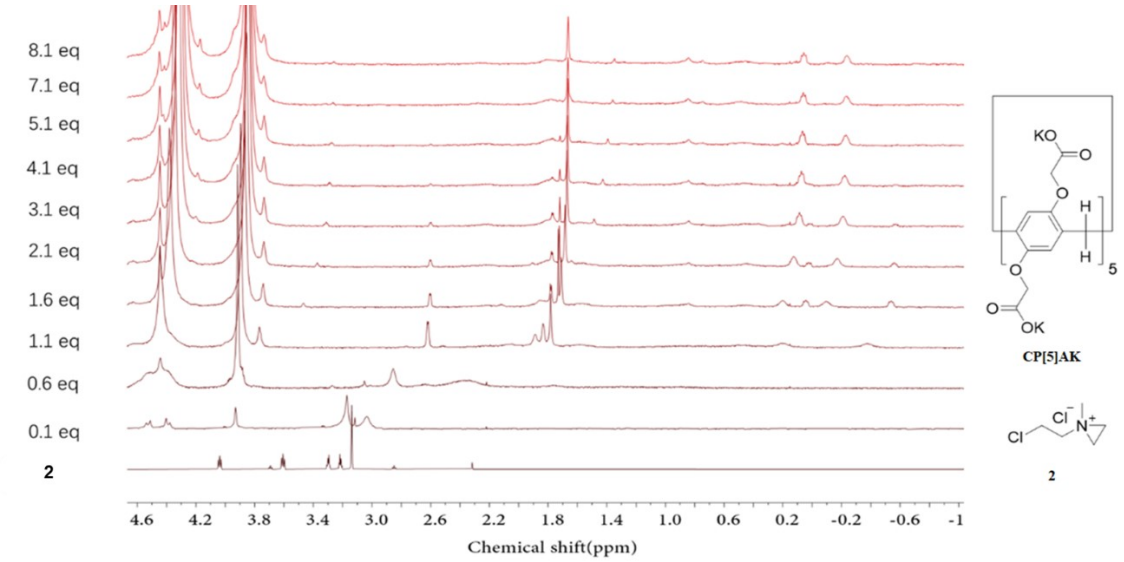

Figure S13. Sections of ^{1}H NMR spectra (600 MHz, 298 K) of a solution of **2** (10.0 mM in D_2O) obtained upon an incremental addition of **CP[5]AK** (0-8.10 equiv.) in D_2O.

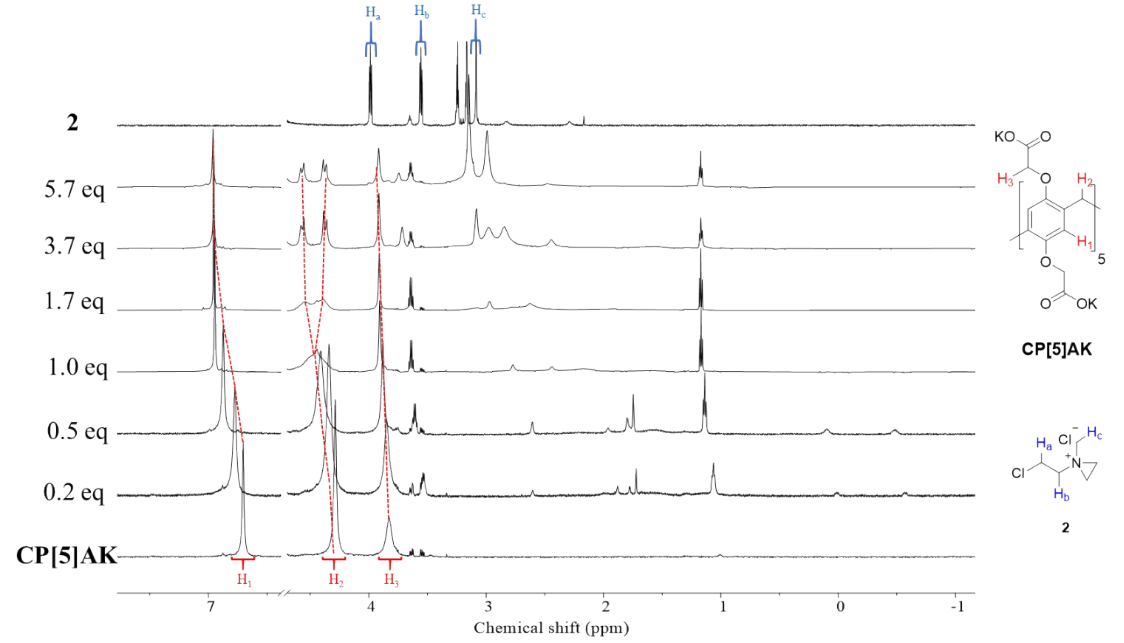

Figure S14. Sections of ^{1}H NMR spectra (600 MHz, 298 K) of a solution of **CP[5]AK** (1.0 mM in D_2O) obtained upon an incremental addition of **2** (0-5.7 equiv.) in D_2O.

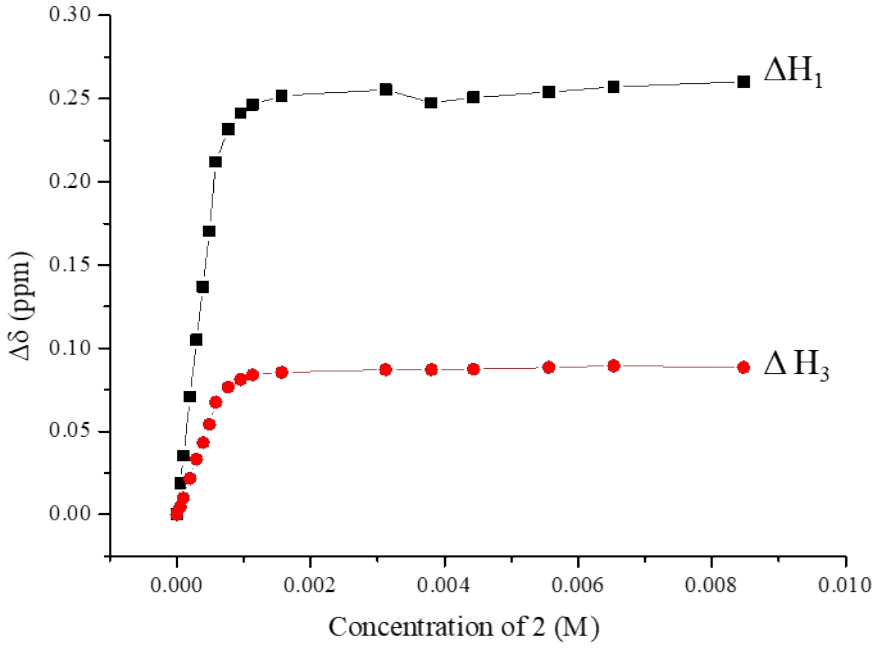

Figure S15. The observed ^{1}H NMR chemical shifts ($\Delta\delta = \delta_{observed} - \delta_{free}$ ppm) of protons in **CP[5]AK** upon an incremental addition of **2** (0-5.7 equiv.) in D_2O.

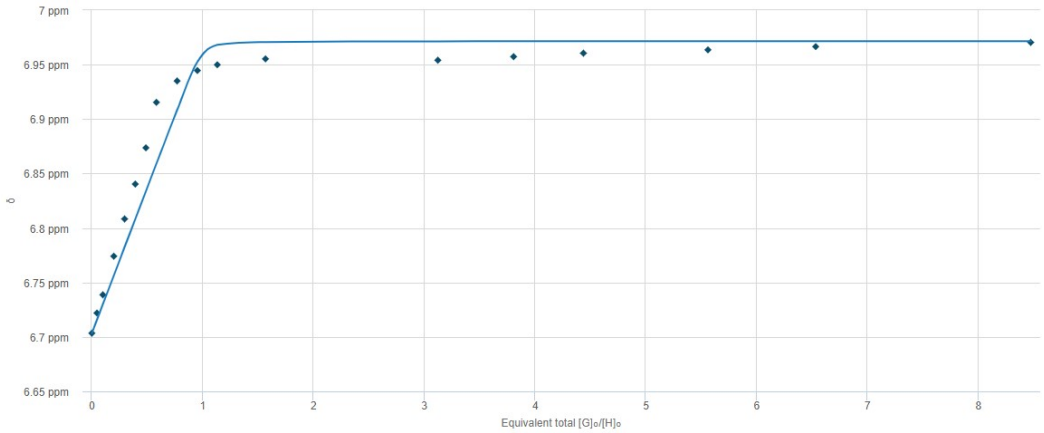

Figure S16. (a) Non-linear least-squares fitting of the chemical shift changes of H_1 during titration experiments of **CP[5]AK** with **2**. (b) the speciation profiles. The chemical shift of H_1 was fitted to a 1:1 (host : guest) binding model to give K_a = 5.45 × 10^5 M^{-1}. All solid lines were obtained from non-linear curve-fitting with the Nelder-Mead method to a 1:1 binding model using the http://supramolecular.org/ web applet.

Temperature (°C)	pH	K_a (M^{-1})	ΔG (kcal/mol)	ΔH (kcal/mol)	ΔS (cal/mol)
10	8.8	(3.47 ± 0.59) × 10^5	-7.08	-7.81	-2.57

25	8.8	(1.51 ± 0.15) × 10^5	-7.07	-7.85	-2.62
37	8.8	(7.04 ± 0.99) × 10^4	-6.88	-7.58	-2.26
25	7.4	(1.84 ± 0.04) × 10^4	-5.82	-8.33	-8.38

Table S1. Thermodynamic parameters of the binding of **CP[5]AK** with **2**.

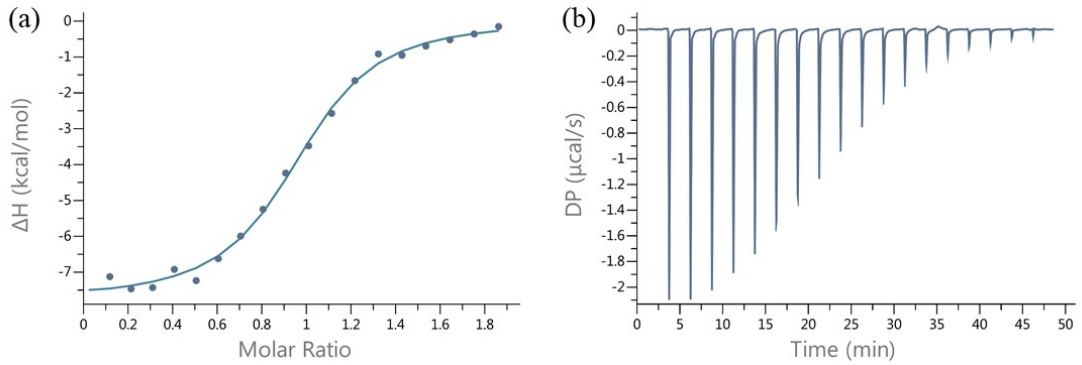

Figure S17. (a) Plot of DP versus time from the titration of a mixture of **CP[5]AK** (100 μM, in H_2O, 10 °C) in the cell with **2** (1.00 mM, in H_2O, 10 °C) in the syringe . (b) plot of the ΔH as a function of molar ratio. The solid line represents the best non-linear fit of the data to a 1:1 binding model (K_a = (3.47 ± 0.59) × 10^5 M^{-1}, ΔH = -7.81 kcal/mol, -TΔS = 0.728 kcal/mol).

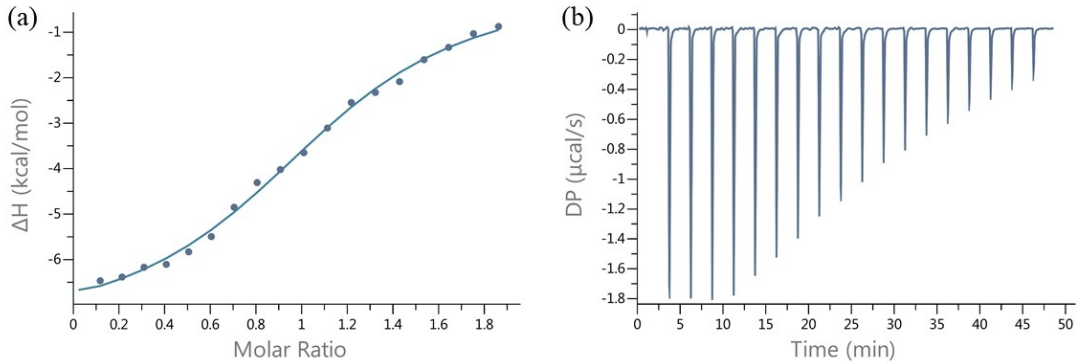

Figure S18. (a) Plot of DP versus time from the titration of a mixture of **CP[5]AK** (100 μM, in H_2O, 37 °C) in the cell with **2** (1.00 mM, in H_2O, 37 °C) in the syringe. (b) plot of the ΔH as a function of molar ratio. The solid line represents the best non-linear fit of the data to a 1:1 binding model (K_a = (7.04 ± 0.99) × 10^4 M^{-1}, ΔH = -7.58 kcal/mol, -TΔS = 0.700 kcal/mol).

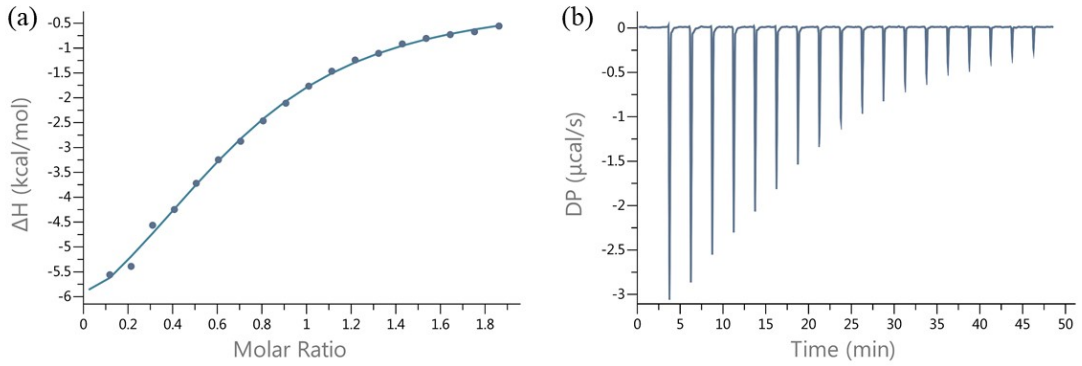

Figure S19. (a) Plot of DP versus time from the titration of a mixture of **CP[5]AK** (100 μM, in PBS, 25 °C) in the cell with **2** (1.00 mM, in PBS, 25 °C) in the syringe. (b) plot of the ΔH as a function of molar ratio. The solid line represents the best non-linear fit of the data to a 1:1 binding model (K_a = (1.84 ± 0.04) × 10^4 M^{-1}, ΔH = -8.33 kcal/mol, -TΔS = 2.5 kcal/mol).

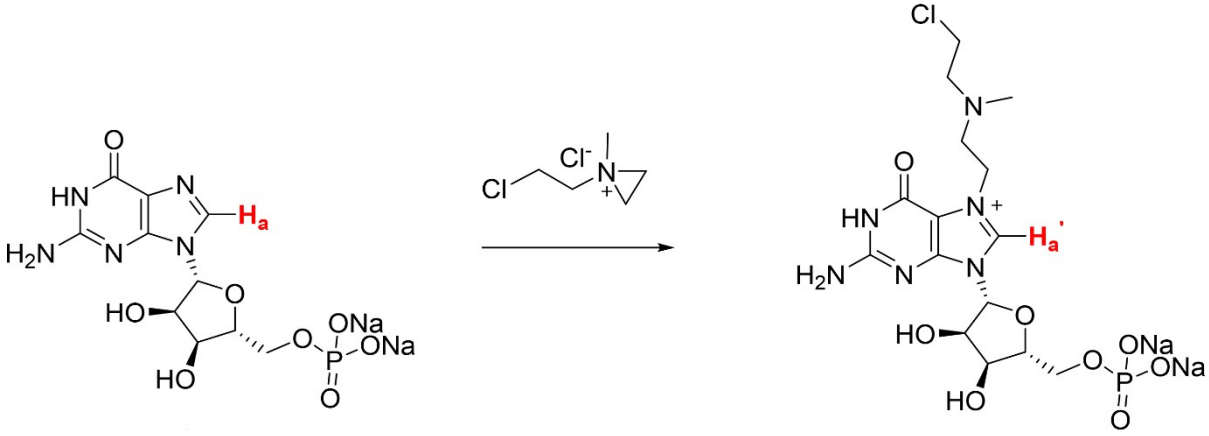

Figure S20. Monoalkylation of guanine disodium nucleotide by **2**.

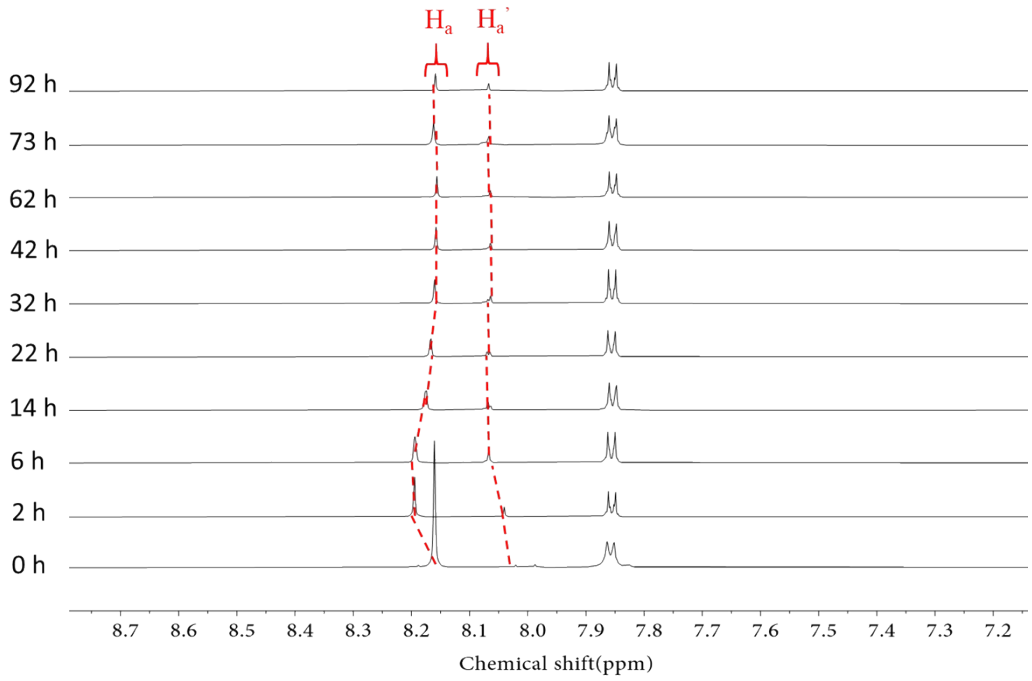

Figure S21. The section of the ^{1}H NMR spectra (600 MHz, 298 K) of **GMP** disodium salt at an initial concentration of 5.00 mM in the presence of **NM** (1.0 equiv.) in D_2O at different time.

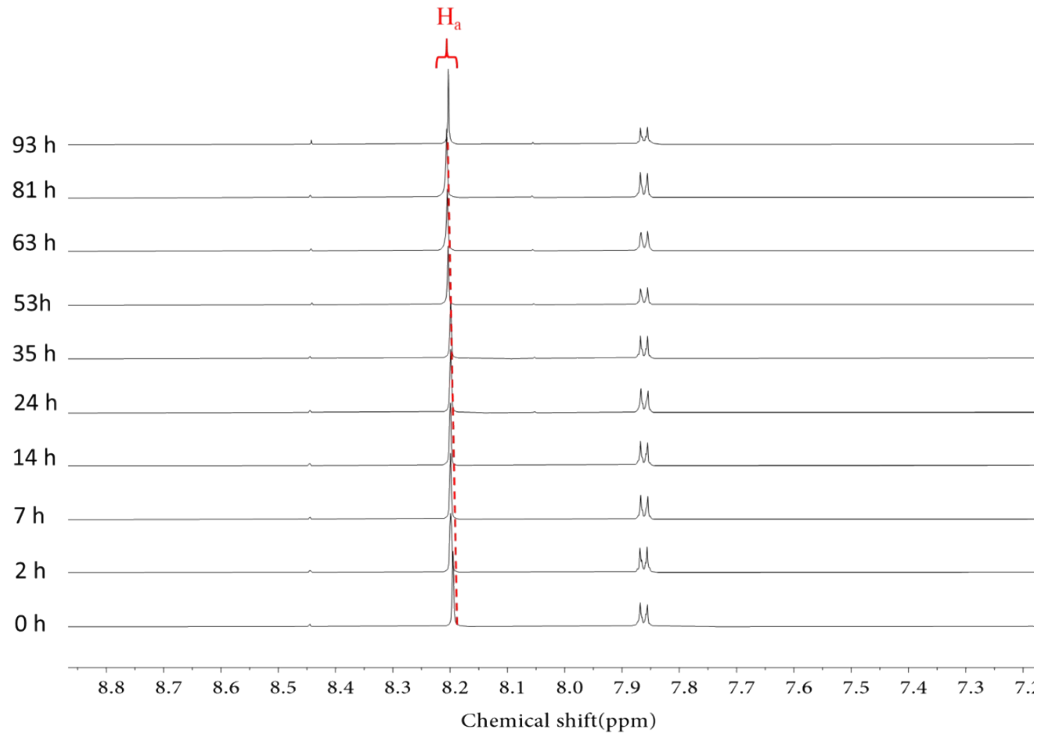

Figure S22. The section of the ^{1}H NMR spectra (600 MHz, 298 K) of **GMP** disodium salt and **NM** at an initial concentration of 5.00 mM in the presence of **CP[5]AK** (1.0 equiv.) in D_2O at different time.

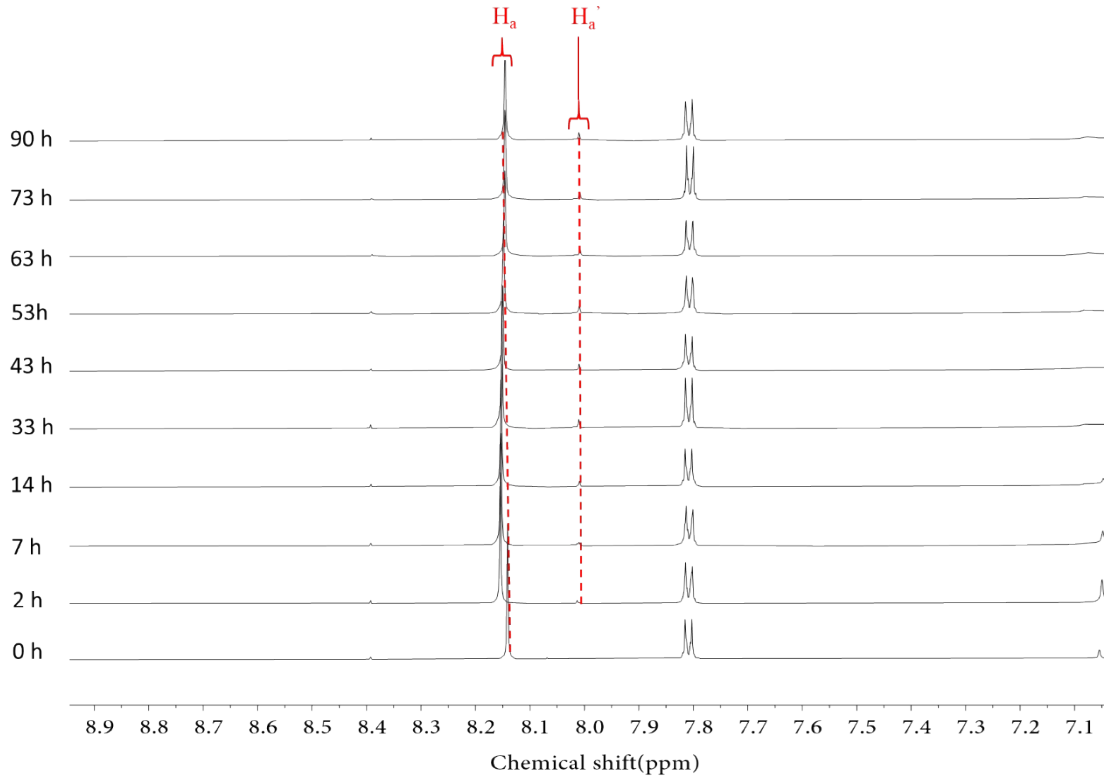

Figure S23. The section of the ^{1}H NMR spectra (600 MHz, 298 K) of **GMP** disodium salt

and **NM** at an initial concentration of 5.00 mM in the presence of **CP[5]AK** (0.5 equiv.) in D_2O at different time.

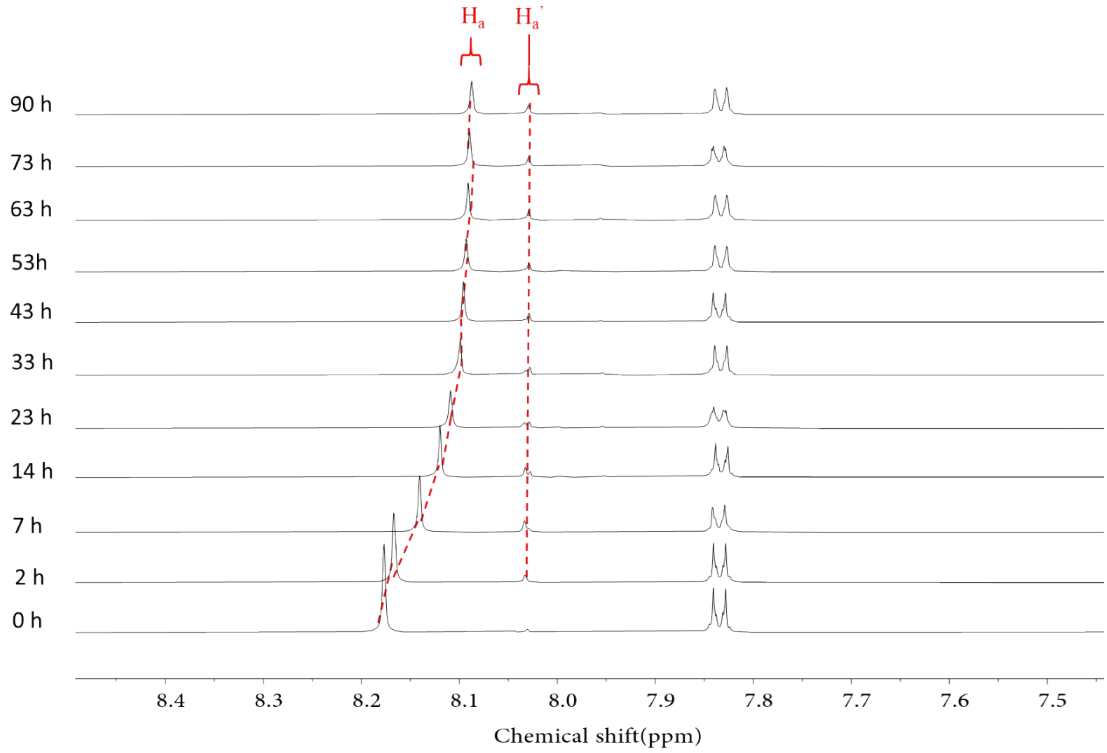

Figure S24. The section of the ^{1}H NMR spectra (600 MHz, 298 K) of **GMP** disodium salt and **NM** at an initial concentration of 5.00 mM in the presence of **CP[5]AK** monomer (5.0 equiv.) in D_2O at different time.

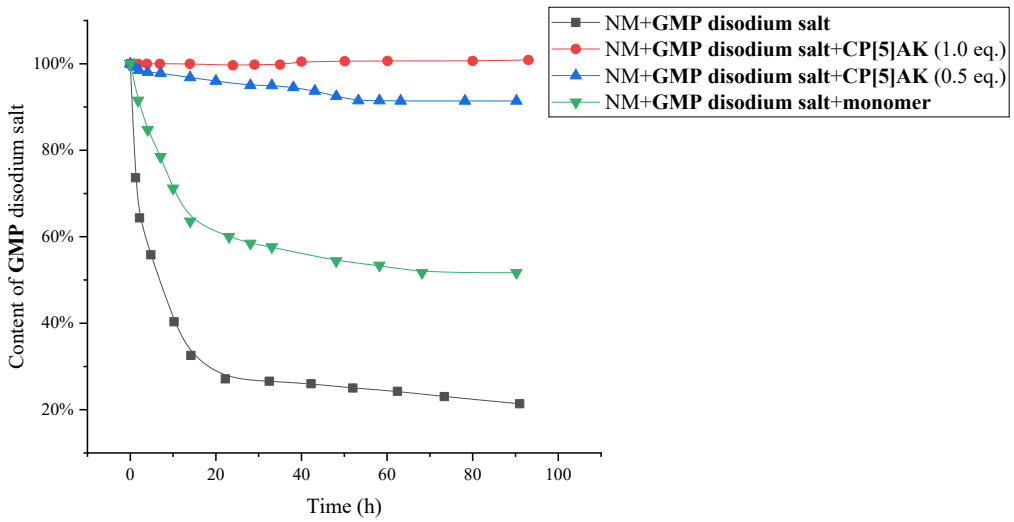

Figure S25. The content of **GMP** disodium salt with time in different experimental groups.

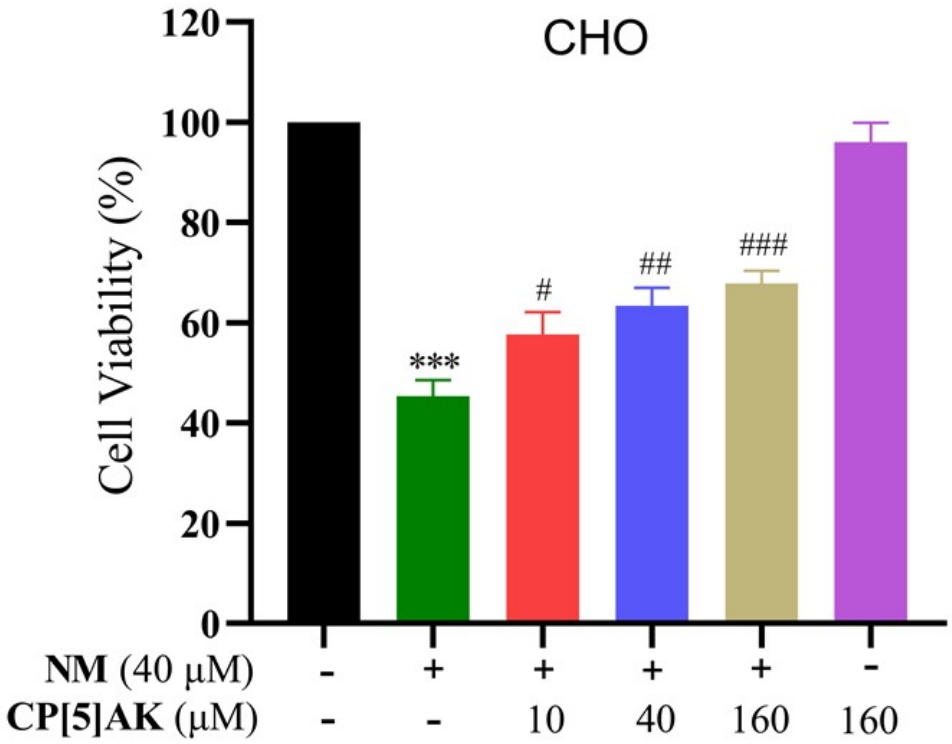

Figure S26. Effects of **CP[5]AK** and **NM** on the cell viability of CHO cells for 48 h. The data are expressed as means ± SD (n = 3). **p* < 0.05, ***p* < 0.01, ****p* < 0.001 compared with the control group. #*p* < 0.05, ##*p* < 0.01, ###*p* < 0.001 compared with the NM treatment group.

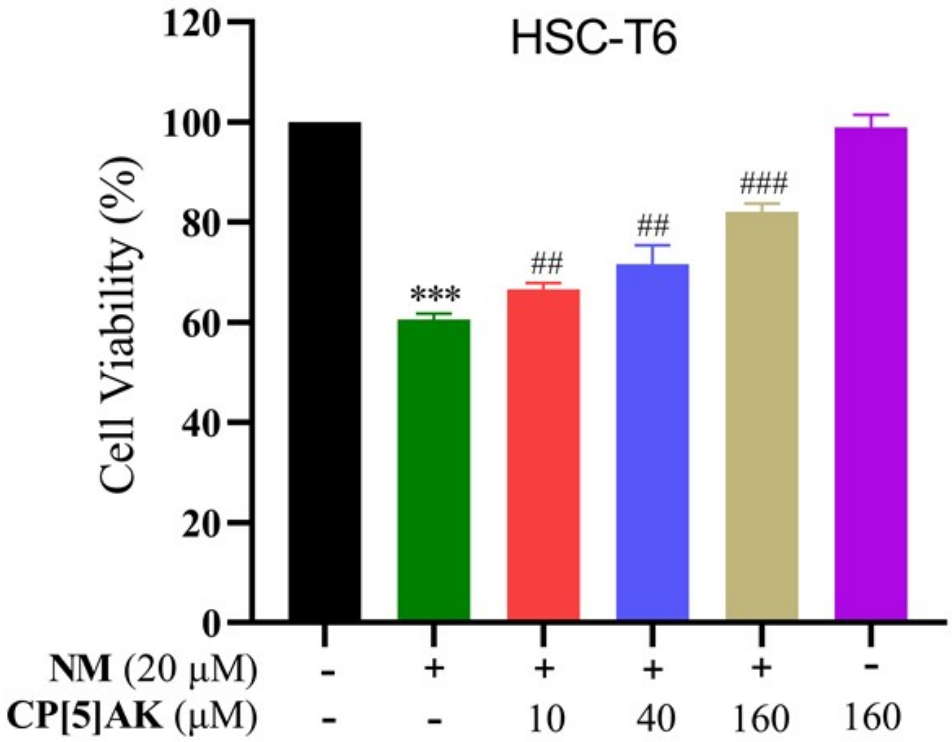

Figure S27. Effects of **CP[5]AK** and **NM** on the cell viability of HSC-T6 cells for 48 h. The data are expressed as means ± SD (n = 3). *p < 0.05, **p < 0.01, ***p < 0.001 compared with the control group. #p < 0.05, ##p < 0.01, ###p < 0.001 compared with the NM treatment group.

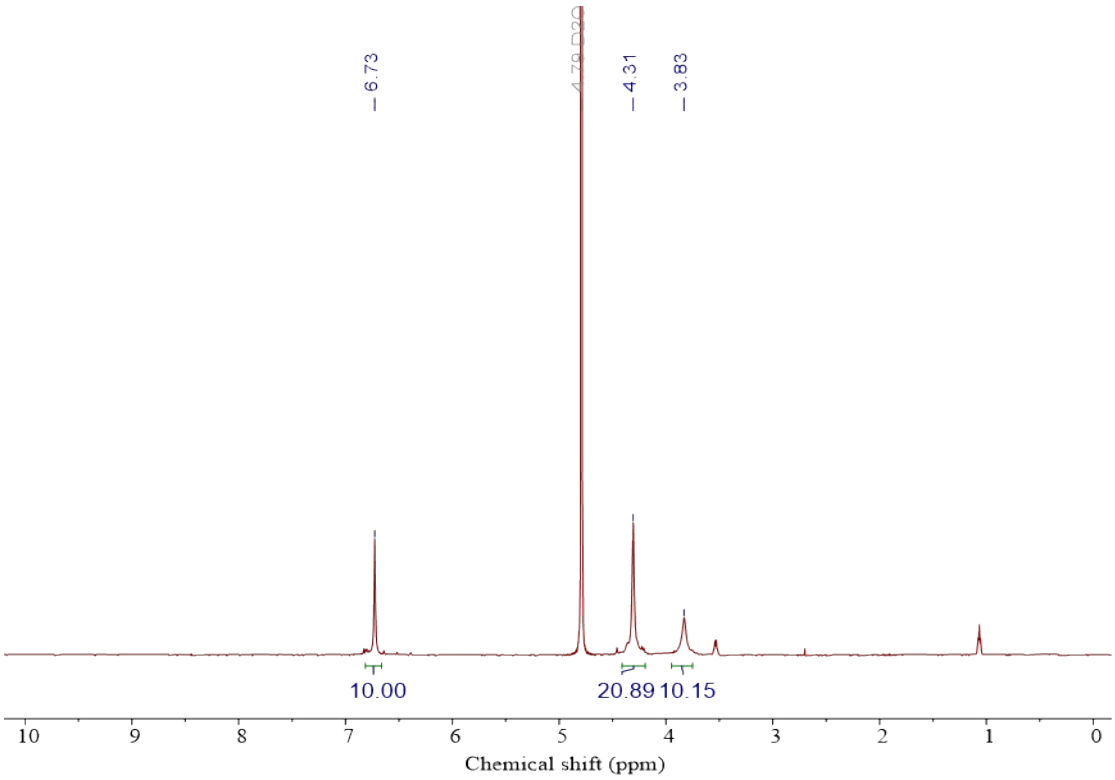

Figure S28. ^{1}H NMR spectrum (D_2O, 298 K, 600 MHz) of **CP[5]AK**.

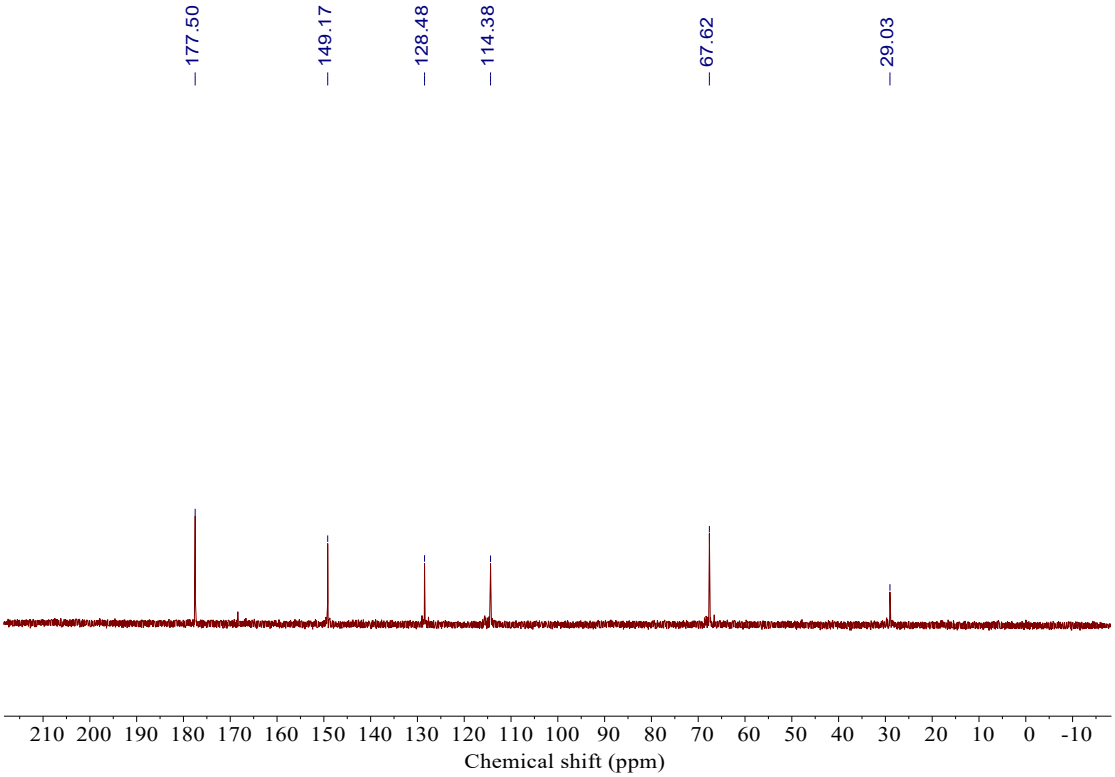

Figure S29. ^{13}C NMR spectrum (D_2O, 298 K, 600 MHz) of **CP[5]AK**.

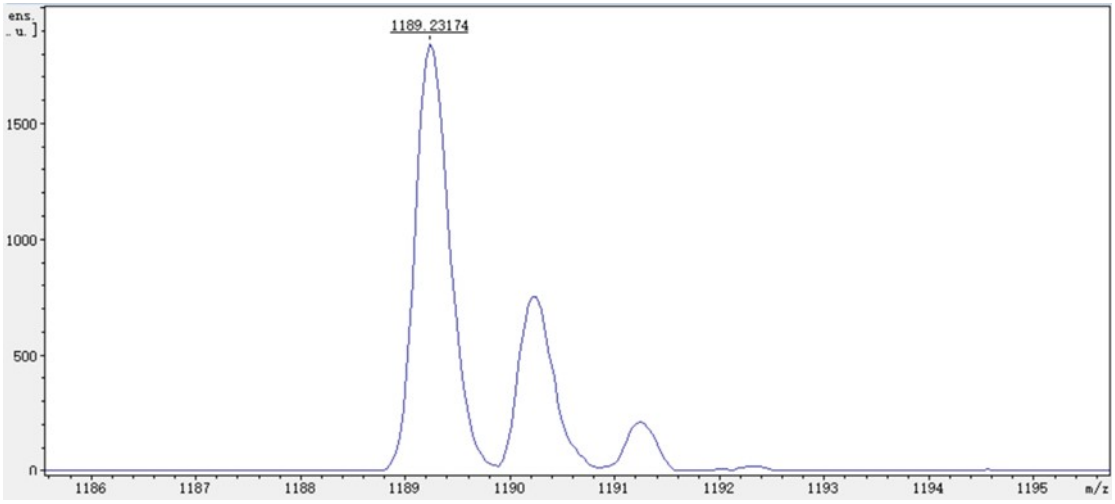

Figure S30. MALDI-TOF mass spectrum of **CP[5]AK** $[M\text{-}10K^{+}+9H^{+}]^{-}$.

References

(1). Frisch, M. J.; Trucks, G. W.; Schlegel, H. B.; Scuseria, G. E.; Robb, M. A.; Cheeseman, J. R.; Scalmani, G.; Barone, V.; Petersson, G. A.; Nakatsuji, H.; Li, X.; Caricato, M.; Marenich, A. V.; Bloino, J.; Janesko, B. G.; Gomperts, R.; Mennucci, B.; Hratchian, H. P.; Ortiz, J. V.; Izmaylov, A. F.; Sonnenberg, J. L.; Williams; Ding, F.; Lipparini, F.; Egidi, F.; Goings, J.; Peng, B.; Petrone, A.; Henderson, T.; Ranasinghe, D.; Zakrzewski, V. G.; Gao, J.; Rega, N.; Zheng, G.; Liang, W.; Hada, M.; Ehara, M.; Toyota, K.; Fukuda, R.; Hasegawa, J.; Ishida, M.; Nakajima, T.; Honda, Y.; Kitao, O.; Nakai, H.; Vreven, T.; Throssell, K.; Montgomery Jr., J. A.; Peralta, J. E.; Ogliaro, F.; Bearpark, M. J.; Heyd, J. J.; Brothers, E. N.; Kudin, K. N.; Staroverov, V. N.; Keith, T. A.; Kobayashi, R.; Normand, J.; Raghavachari, K.; Rendell, A. P.; Burant, J. C.; Iyengar, S. S.; Tomasi, J.; Cossi, M.; Millam, J. M.; Klene, M.; Adamo, C.; Cammi, R.; Ochterski, J. W.; Martin, R. L.; Morokuma, K.; Farkas, O.; Foresman, J. B.; Fox, D. J. *Gaussian 09 Rev. A.02*, Gaussian 09 (Gaussian, Inc., Wallingford CT, 2009).

(2). Lu, T.; Chen, F. W., Multiwfn: A Multifunctional Wavefunction Analyzer. *J. Comput. Chem.* **2012**, *33*(5), 580-92.

(3). Li, H.; Chen, D.-X.; Sun, Y.-L.; Zheng, Y. B.; Tan, L.-L.; Weiss, P. S.; Yang, Y.-W., Viologen-Mediated Assembly of and Sensing with Carboxylatopillar[5]arene-Modified Gold Nanoparticles. *J. Am. Chem. Soc.* **2013**, *135*(4), 1570-1576.

(4). Li, X.-S.; Li, Y.-F.; Wu, J.-R.; Lou, X.-Y.; Han, J.; Qin, J.; Yang, Y.-W., A color-tunable fluorescent pillararene coordination polymer for efficient pollutant detection. *J. Mater. Chem. A* **2020**, *8*(7), 3651-3657.